

# Constraints on stability and renormalization group flows in nonequilibrium matter

Yu-Hsueh Chen and Tarun Grover

*Department of Physics, University of California at San Diego, La Jolla, California 92093, USA*

We derive constraints on renormalization group (RG) flows and stability of phases in nonequilibrium systems using quantum information inequalities. These constraints involve conditional mutual information (CMI), which quantifies correlations between spatially separated regions not mediated by their surroundings. First, assuming CMI is UV finite, we show that the scaling function associated with CMI is monotonic along the RG flow. This implies a non-perturbative stability criterion: a fixed point with smaller CMI cannot be destabilized toward one with larger CMI. Second, we bound the CMI of a convex mixture of states in terms of the CMI of individual components. We use this inequality to infer perturbative stability of spontaneous symmetry breaking states against quantum channels that explicitly break symmetry. We illustrate these constraints through several examples, including decoherence-driven transitions in classical symmetry-broken states, strong-to-weak symmetry breaking criticality in two dimensions, and even transitions in pure quantum states. We also discuss implications for classical nonequilibrium steady states.

**Introduction.** Non-perturbative constraints on renormalization group (RG) flows of interacting theories [1–9] have been a powerful tool in exploring phases and phase diagrams of strongly interacting systems (see, e.g.,[10–17]). A striking result is that such constraints can often be derived as a consequence of information theoretic inequalities [8, 18–23]. Ideas from quantum information theory have been used to also derive general constraints on the structure of gapped ground states and conformal field theories [24–30]. It is natural to wonder if the nexus of ideas from information theory and many-body physics can also constrain the landscape of phenomena in more general settings, e.g., an out-of-equilibrium steady state of a long-time evolved quantum system. In this work, we will pursue this direction and employ quantum information inequalities to derive consequences for the renormalization group flow and stability of nonequilibrium systems. We will discuss several applications, ranging from decoherence induced phase transitions to stability of spontaneous symmetry breaking against perturbations that explicitly break the symmetry, and also to classical nonequilibrium systems.

The object of our central interest will be conditional mutual information (CMI), defined as  $I(A : C|B) = S(AB) + S(BC) - S(B) - S(ABC)$ , where  $S(X)$  denotes von Neumann entropy for the density matrix  $\rho_X$  associated with region  $X$ . CMI is positive due to strong subadditivity (SSA) and it captures correlations between subregions  $A$  and  $C$  that are not mediated by  $B$ . In a large class of systems, CMI decays exponentially with the separation  $l_B$  between  $A$  and  $C$ :  $I \sim e^{-l_B/\xi_M}$  where  $\xi_M$  is called the *Markov length*. As recently discussed [31, 32], Markov length plays an essential role in defining mixed state phases of matter [33, 34]. Notably, for Gibbs states of local Hamiltonians at a non-zero temperature, Markov length is finite [35] (and is exactly zero for commuting, local Hamiltonians [36–38]).

In the following, we will discuss two results. The first result is an inequality for CMI along an RG flow, while the second result bounds the CMI of a convex mixture of states in terms of the CMI of individual components.

**Monotonicity of CMI under RG.** Consider a system in  $d$  spatial dimensions described by a state  $\rho(t)$  near a critical point, where  $t$  is a dimensionless scaling variable with RG eigenvalue  $1/\nu$ . The full system is of size  $L_{\parallel} \times l^{d-1}$  where  $L_{\parallel} = \alpha l$  and  $\alpha$  is any fixed  $O(1)$  number. We impose open boundary conditions along the  $\parallel$  direction. We further assume that the bulk of the system is translationally invariant along  $\parallel$  direction and neglect any boundary effects (we will be primarily interested in the limit  $l \rightarrow \infty$ ). The system is partitioned into three regions,  $A$ ,  $B$ , and  $C$ , where  $B$  is a slab of size  $l_B \times l^{d-1}$  that separates  $A$  and  $C$  which have equal sizes [see Fig.1(a)].  $l$  and  $l_B$  are both dimensionless lengths measured in units of the lattice spacing  $a$ , which serves as the UV cutoff. We will denote CMI  $I(A : C|B)$  as  $I(l|l_B, t)$ . SSA implies that CMI is monotonically decreasing with increasing  $l_B$ :

$$I(l|l_B + 2\Delta, t) \leq I(l|l_B, t), \quad \forall \Delta > 0, \quad (1)$$

The proof is straightforward: the difference  $\Delta I = I(A : C|B) - I(A' : C'|B')$ , illustrated in Fig. 1(a), can itself be expressed as a CMI [39] and is therefore non-negative. Let's now consider the limit  $l/l_B \rightarrow \infty, l|t|^{\nu} \rightarrow \infty$ . In this limit, on dimensional grounds, the CMI  $I(\infty|l_B, t)$  may depend on two dimensionless variables,  $l_B$  and  $l_B^{1/\nu} t \equiv x$ . However, assuming CMI is finite in the scaling limit  $l_B, |t|^{-\nu} \gg 1$  (“UV finite”), it can depend only on  $x$ . Eq. (1) then implies:

$$\frac{df(x)}{dx} \leq 0, \quad (2)$$

where  $I(\infty|l_B, t) \equiv f(tl_B^{1/\nu})$ . This is our first main result. An analogous constraint holds in the presence of multiple relevant scaling parameters  $\{t_i\}$ . Implicit in Eq.(2) is the assumption that the function  $f(x)$  is continuous and at least once differentiable in the domain of our interest, which we will take to be  $|x| \in (0, \infty)$ . For finite  $l$ , the CMI generically also depends on the ratio  $l/l_B$ . In one spatial dimension, a direct application of SSA shows that

the CMI can only increase as  $l$  is increased at fixed  $l_B$ . If the CMI takes the form  $I(l|l_B, t) = [(\alpha l - l_B)/l_B]^\eta f(x)$ , this implies that the anomalous dimension  $\eta$  must be non-negative (here  $(\alpha l - l_B)/l_B \ll 1$ ). We next briefly discuss the assumption of UV finiteness of CMI.

In a system described by a local space-time action, the UV-divergent contributions to entropies defining CMI are expected to be *local functionals* of the entangling boundary [40–47], and are therefore expected to cancel in the combination defining CMI [48]. Indeed, for ground states of quantum field theories, there is substantial evidence for this statement based on general arguments [40–47] and also explicit calculations [49–53]. Although most of these works focus on ground states of local Hamiltonians, the arguments leading to the conclusion rely essentially on the fact that the system admits a well defined continuum limit governed by an action local in space-time. Therefore, we anticipate that this conclusion holds also for the CMI of nonequilibrium systems whose density matrices can be expressed in terms of a local space-time action e.g. Martin-Siggia-Rose-Janssen-De Dominicis (MSRJD) functional [54–57] for the steady state of a locally-interacting classical many-body system. We will provide examples later from nonequilibrium systems that substantiate this expectation. It is also worth noting that known examples where CMI is *not* UV finite [44, 58] all involve systems that do not admit a conventional thermodynamic limit, notably fractonic and subsystem symmetric systems [59–65]. In such systems, RG itself is rather unconventional [66–68], and we exclude such systems from further discussion (nonetheless, Eq.(1) is always true, and may still be constraining).

Let us derive several implications of the inequality  $d\text{CMI}(x)/d|x| \leq 0$ . The key point is that in an RG flow,  $\text{CMI}(0 < |x| \ll 1)$  will be representative of the UV fixed point, while  $\text{CMI}(|x| \gg 1)$  will correspond to that of the IR fixed point. In principle,  $\text{CMI}(x = 0)$  may differ from  $\lim_{|x| \rightarrow 0^+} \text{CMI}(x)$ . In the following, we assume that  $\text{CMI}(x)$  is continuous at  $x = 0$  along the RG-relevant flow of this fixed point. Let us consider perturbing a Gibbs state of a local Hamiltonian with an arbitrary channel of strength  $p$ . Such a state may correspond to a finite- $T$  critical point and can therefore possess relevant RG directions. As recently shown [35], it has a finite Markov length: CMI decays as  $I \sim I_0 e^{-l_B/\xi}$  where  $\xi$  is the Markov length corresponding to this state, and  $I_0$  is a finite nonzero constant. Therefore, at the corresponding RG fixed point ( $l_B/\xi \rightarrow \infty$ ),  $I = 0$ . By monotonicity, any perturbation of this fixed point cannot destabilize the system toward a state with nonzero CMI. A similar conclusion was recently derived for specific channels using microscopic considerations [69]. Another consistency check is that the 1+1-D KPZ fixed point [70] can be obtained by perturbing a Gaussian Gibbs state by a relevant non-linear term that breaks detailed balance. Therefore, the steady state of the 1+1-D KPZ must also be a Gibbs state of a local Hamiltonian, which is indeed the case [70]. A more non-trivial application is

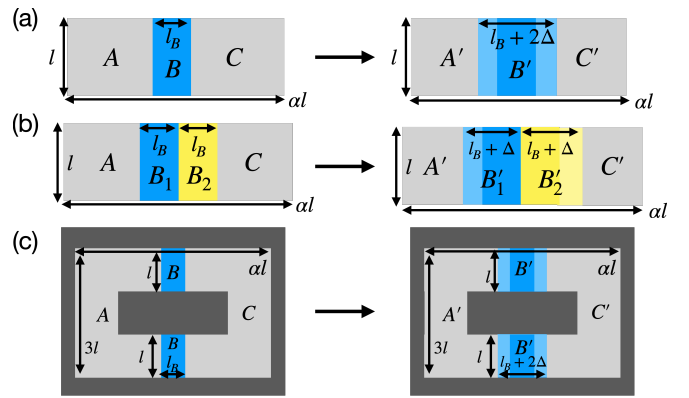


FIG. 1. We primarily focus on the geometry shown in (a), where the full system in  $d$  spatial dimensions of size  $\alpha l \times l^{d-1}$  ( $\alpha$  is an arbitrary order one number) is partitioned into three regions:  $A$ ,  $B$ , and  $C$ .  $B$  is a slab of size  $l_B \times l^{d-1}$  that separates  $A$  and  $C$  of equal sizes. (b), (c): Other geometries for which our results can be straightforwardly generalized to (see main text).

the detailed-balance-breaking perturbation to the Gaussian scalar field theory [71] which destabilizes it towards a nonequilibrium steady state studied in Ref.[72, 73]. Again assuming our aforementioned assumptions hold, the steady state at this non-trivial fixed point must have zero CMI and is therefore expected to be Gibbs state of a local Hamiltonian due to Hammersley–Clifford theorem [36]. More generally, a fixed point with lower CMI is stable against perturbations that would drive it toward one with larger CMI. For example, although a  $\mathbb{Z}_2$  strong-to-weak spontaneously symmetry-breaking (SWSSB) fixed point [74, 75], which has CMI  $\log 2$ , can be driven to a trivial state with zero CMI by an infinitesimal perturbation, it is impossible to drive it instead to a  $\mathbb{Z}_4$  SWSSB state with CMI  $\log 4$  (for completeness, we provide a brief review of SWSSB in Ref.[39]).

Conversely, if the IR fixed point has infinite Markov length, the UV fixed point cannot be a Gibbs state of a local Hamiltonian. This observation has an immediate implication for the exotic multicritical point identified in Ref. [76], which flows to the 1+1-D directed percolation (DP) critical point on the one side of the phase diagram, and to the 1+1-D KPZ critical point on the other. As shown recently [77], the 1+1-D DP critical point has infinite Markov length. Therefore, although the critical field theory for this multicritical point remains unknown, the corresponding state cannot be a Gibbs state of a local Hamiltonian and must have an infinite Markov length. As an aside, Ref.[77] related the CMI  $I(A : C|B)$  at the 1+1-D compact DP fixed point to the escape probability of a domain wall from region  $B$ , again illustrating the inequality  $\partial I / \partial l_B \leq 0$ . The scaling form  $I(\infty|l_B, \{t_i\}) = f(\{t_i l_B^{1/\nu}\})$  was also confirmed analytically.

While we focus primarily on the geometry shown in Fig. 1(a), our results generalize straightforwardly to other geometries. For instance, Fig. 1(b) partitions

the system into four regions  $A$ ,  $B_1$ ,  $B_2$ , and  $C$ , where  $B_{1,2}$  are slabs of size  $l_B \times l^{d-1}$ . The same arguments show that  $I(A : C|B_1) \equiv I(\infty|l_B, t) = f(tl_B^{1/\nu})$  satisfies  $df(x)/d|x| \leq 0$ . One application concerns RG flows involving symmetry-protected topological (SPT) and SWSSB states. In the limit  $l \rightarrow \infty$ , for this geometry, the fixed point of the one-dimensional  $\mathbb{Z}_2 \times \mathbb{Z}_2$  SPT phase has CMI equal to  $2 \log 2$  [78], whereas any SWSSB fixed point has zero CMI. This rules out a direct instability of SWSSB states toward a  $\mathbb{Z}_2 \times \mathbb{Z}_2$  SPT phase.

Another useful choice is the Levin–Wen geometry [79] shown in Fig.1(c), commonly used to extract the topological entanglement entropy (TEE) [79, 80]. A similar reasoning yields the scaling form  $I(\infty|l_B, t) = f(tl_B^{1/\nu})$ , with  $df(x)/d|x| \leq 0$ . This result is reminiscent of the  $F$ -theorem [8], which states that along RG flows between 2+1-D CFTs, the subleading, universal constant term in the entanglement entropy of a circular region—identified with the TEE in topologically ordered systems—decreases from the UV to the IR fixed point. Unlike the  $F$ -theorem, our setup does not assume Lorentz invariance. At the same time, while  $F$  is an  $O(1)$  universal constant for a given CFT, CMI for Fig.1(c) generically depends on the geometry, and the bound may be trivially satisfied—e.g., if the UV fixed point is a 2+1-D CFT, one expects that CMI will be proportional to  $l/l_B$  [41, 81, 82], and since  $l/l_B \gg 1$ , the bound is not constraining for the IR. Nevertheless, this setup constrains RG flows involving mixed state(s) where the  $F$ -theorem does not apply. For instance, a  $\mathbb{Z}_n$  SWSSB state has zero CMI for this geometry, implying that it cannot become unstable towards an IR fixed point with either a classical or quantum topological memory, both of which have a non-zero Levin–Wen CMI [32, 79].

**Bounding CMI via convex decomposition.** Next, we will employ SSA to derive a bound on CMI for a convex sum of density matrices in terms of the CMI of individual components. Consider any convex decomposition  $\rho = \sum_\alpha p_\alpha \rho_\alpha$ . Using SSA, one finds [39]:

$$I_\rho(A : C|B) \leq \sum_\alpha p_\alpha I_{\rho_\alpha}(A : C|B) + S_\sigma(D|B), \quad (3)$$

where  $\sigma = \sum_\alpha p_\alpha |\alpha\rangle\langle\alpha|_D \otimes \rho_\alpha$ . Eq.(3) can be thought of as the analog Holevo bound,  $S(\rho) \leq H(\{p_\alpha\}) + \sum_\alpha p_\alpha S(\rho_\alpha)$ , for CMI.

Eq. (3) implies that if each  $\rho_\alpha$  has finite Markov length and  $S_\sigma(D|B)$  decays exponentially in  $l_B$ , then  $\rho$  also has a finite Markov length. This observation allows one to assess robustness of spontaneous symmetry-breaking against generic perturbations, including those that break the symmetry explicitly. As a concrete example, consider the classical mixture  $\rho_0 = \frac{1}{2}(|\uparrow\rangle\langle\uparrow|)^N + \frac{1}{2}(|\downarrow\rangle\langle\downarrow|)^N$  which describes the zero-temperature limit of the classical Ising model in any dimension and has long range  $\langle Z_i Z_j \rangle$  correlations. Applying a  $p$ -bounded channel  $\mathcal{E}$  of

strength  $p$  [83] to  $\rho_0$  leads to a natural decomposition,

$$\rho = \frac{1}{2} \mathcal{E}[ (|\uparrow\rangle\langle\uparrow|)^{\otimes N} ] + \frac{1}{2} \mathcal{E}[ (|\downarrow\rangle\langle\downarrow|)^{\otimes N} ]. \quad (4)$$

Under the assumption that a trivial product state (e.g.,  $(|\uparrow\rangle\langle\uparrow|)^N$ ) remains robust under the action of  $\mathcal{E}$ , the first term in Eq. (3) decays exponentially with  $l_B$  for sufficiently small  $p$ . This assumption is equivalent to requiring that the trivial phase corresponding to a product state is a stable phase of matter, which has been proven in Ref. [84] for a broad class of channels. Moreover, Fano’s inequality [85] implies that  $S_\sigma(D|B)$  also decays exponentially for any  $p$ -bounded local channel with sufficiently small  $p$ . Therefore, for sufficiently small  $p$ , the Markov length remains finite and the decohered density matrix is in the same phase of matter as  $\rho_0$  [31, 32]. We briefly comment on generalization to other binary classical codes in Ref. [39].

We will now consider a few additional applications/demonstrations of our general results.

**Illustration 1: Stability of classical SSB and its RG flow.** We study a simple model illustrating all inequalities discussed above. We subject the state  $\rho_0 = \frac{1}{2}(|\uparrow\rangle\langle\uparrow|)^l + \frac{1}{2}(|\downarrow\rangle\langle\downarrow|)^l$  in  $d = 1$  to a channel  $\mathcal{E}(p)$  that independently flips each  $\downarrow$  spin with probability  $p$  while leaving  $\uparrow$  spins unchanged. This produces a one-parameter family of mixed states  $\rho(p) = \frac{1}{2}(|\uparrow\rangle\langle\uparrow|)^l + \frac{1}{2}[(1-p)|\downarrow\rangle\langle\downarrow| + p|\uparrow\rangle\langle\uparrow|]^l$ . We first note that  $\rho(p)$  is not the Gibbs state of any local Hamiltonian: the probability of observing  $|\uparrow\rangle^\Lambda$  in any finite region  $\Lambda$  of  $\rho(p)$  exceeds  $1/2$ , violating the alignment-suppression property of finite-temperature Gibbs states [86, 87]. Since  $\rho(p) = \mathcal{E}(p)[\rho_0]$ , with  $\mathcal{E}(p)$  an  $O(1)$ -depth local channel, establishing that  $\rho(p)$  has finite Markov length suffices to guarantee a reverse short-depth local channel  $\mathcal{E}^{-1}$  such that  $\mathcal{E}^{-1}[\rho(p)] = \rho_0$  [31, 32]. As an aside, let  $T$  be any  $\mathbb{Z}_2$ -symmetric channel whose steady state is  $\rho_0$ . The existence of  $\mathcal{E}^{-1}$  then allows one to construct a local channel  $\mathcal{E}T\mathcal{E}^{-1}$  whose steady state is  $\rho(p)$ —a *state with long-range order, but without Ising symmetry*, i.e.,  $\prod_i X_i \rho(p) \prod_i X_i \neq \rho(p)$  [88]. This is reminiscent of Toom’s automata [89, 90].

Let’s employ Eq. (3) to show that  $\rho(p)$  is two-way connected to  $\rho_0$  for sufficiently small  $p$ . Since both  $\mathcal{E}[ (|\uparrow\rangle\langle\uparrow|)^l ]$  and  $\mathcal{E}[ (|\downarrow\rangle\langle\downarrow|)^l ]$  are product states, the first term on the right-hand side of Eq. (3) vanishes. Consequently,  $I_\rho(A : C|B)$  decays exponentially whenever  $S_\sigma(D|B)$  does, which holds for any  $p$ -bounded noise with sufficiently small  $p$  [91]. We next compute the CMI of  $\rho$  explicitly in the limit  $l \rightarrow \infty$  to illustrate that the associated scaling function is monotonic. A direct calculation yields  $I(\infty|l_B, p) = \frac{1}{2}(1 + p^{l_B}) \log(1 + p^{l_B}) - \frac{1}{2}p^{l_B} \log(p^{l_B})$ . In the limit  $\epsilon \equiv (p-1) \rightarrow 0^-$  and  $l_B \rightarrow \infty$  with  $x = \epsilon l_B$  held fixed, one finds

$$I(\infty|l_B, p) \approx f(x) \equiv \frac{1}{2}[(1 + e^x) \log(1 + e^x) - x e^x]. \quad (5)$$

This identifies  $p_c = 1$  and the correlation-length exponent

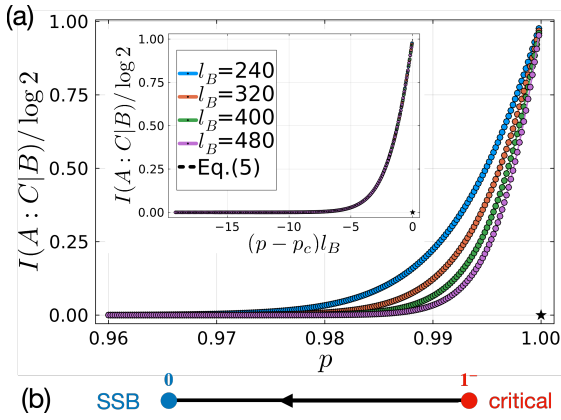


FIG. 2. (a) The conditional mutual information(CMI)  $I(A : C|B) = I(l|l_B, p)$  of the mixed state discussed in Illustration 1 as a function of  $p$  for various  $l_B$  with  $l = 10^8 (\approx \infty)$ . The inset shows the data collapse of the scaling ansatz  $I(l|l_B, p) = f[(p - p_c)l_B^{1/\nu}]$  with  $p_c = 1$  and  $\nu = 1$ . (b) The corresponding RG flow.

$\nu = 1$ , and more importantly shows that  $I(\infty|l_B, p)$  is UV finite. The scaling function  $f(x)$  is readily verified to be monotonically increasing for  $x \in (-\infty, 0)$  [see Fig. 2(a)].

We now analyze  $f(x)$  in the critical and stable regimes. When  $x$  approaches  $0^-$ , one finds  $I(\infty|l_B, p) \approx \log 2(1 + x/2)$ , while for  $x \ll 0$ ,  $I(\infty|l_B, p) \approx e^x(1 - x)/2$ , which vanishes exponentially as  $x \rightarrow -\infty$ ; see Fig. 2(a). The limit  $x \rightarrow 0$  is singular, since  $I$  drops discontinuously to zero at  $x = 0$ . Accordingly, the UV fixed point of the RG flow in Fig. 2(b) sits at  $x = 0^-$ . This is expected because  $\rho(p = 1)$  is a product state and cannot be destabilized towards a symmetry broken state.

Finally, for  $l = l_B + 2r$  with finite  $r$ , we find  $I(l_B + 2r|l_B, p) = (r/l_B)^\eta f(x)$  with anomalous dimension  $\eta = 2 > 0$  [39], consistent with the aforementioned SSA constraint that the CMI is monotonically decreasing under increasing  $l$  while keeping  $l_B$  fixed. We also consider a more general channel that flips a  $\downarrow(\uparrow)$  spin with probability  $p(q)$  [39]; the case  $p = q$  was also studied previously in Ref.[92]. While most features persist from the  $q = 0$  case, we find that the correlation-length exponent is  $\nu = 2$  for  $q \neq 0$ , in contrast to  $\nu = 1$  for  $q = 0$ .

**Illustration 2: CMI of TFIM.** The above constraints apply also to pure states. Let's consider  $ABC$  spanning the entire system so that the CMI reduces to the mutual information  $I(A : C)$ . As an illustration, we compute the CMI of the ground state of the  $(1+1)$ D transverse-field Ising model (TFIM) with Hamiltonian  $H = -\sum_j Z_j Z_{j+1} - h \sum_j X_j$ , which is efficiently accessible by mapping to free fermions. We choose the system size as  $l = 12/|h - h_c|^\nu + 1$ , with  $\nu = 1$  and  $h_c = 1$ , which is sufficiently large that the CMI is well described by the scaling form, even though strict validity requires  $l \rightarrow \infty$ .

Fig. 3(a) shows the CMI as a function of  $l_B$  for several values of  $h$ , while the inset plots it as a function of  $x = (h - h_c)l_B^{1/\nu}$ , demonstrating the scaling form  $I(A : C|B) = f(x)$ .

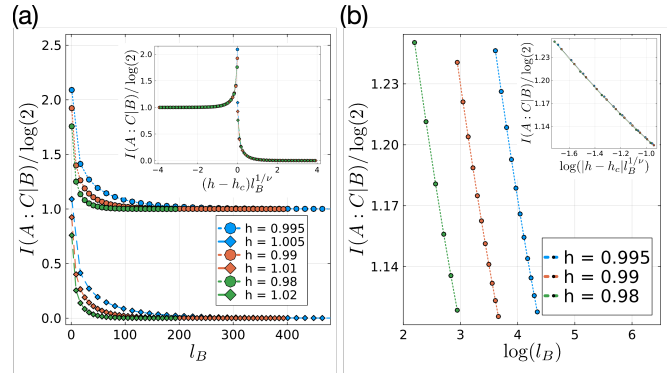


FIG. 3. (a) The CMI of the TFIM as a function of  $l_B$  for several values of  $h$ . The inset shows a data collapse using the scaling ansatz  $I(A : C|B) = f[(h - h_c)l_B^{1/\nu}]$  with  $h_c = 1$  and  $\nu = 1$ . (b) The CMI as a function of  $\log(l_B)$  for several values of  $h < h_c$ . The insets show the same data plotted as a function of  $\log(|h - h_c| l_B^{1/\nu})$ .

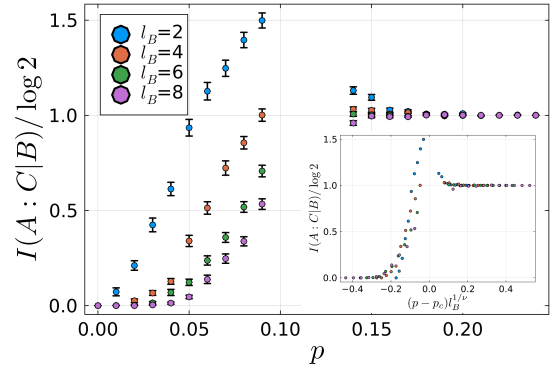


FIG. 4. The CMI for the trivial-to-SWSSB transition in two spatial dimension as a function of  $p$  for various  $l_B$ . The inset shows the data collapse with the scaling ansatz  $I(A : C|B) = f[(p - p_c)l_B^{1/\nu}]$  with  $p_c = 0.109$  and  $\nu = 1.5$ .

$C|B) = f(x)$ . One observes that  $f(x)$  is monotonically decreasing (increasing) for  $x \in (0, \infty)$  ( $x \in (-\infty, 0)$ ). Further, when  $x \rightarrow 0^-$ ,  $f(x) \rightarrow -(c/3) \log(|x|) + \log 2$  diverges logarithmically with central charge  $c = 1/2$ —the constant term is well-defined since  $f(x)$  is independent of the UV cutoff. This behavior follows analytically from Ref. [93], and is confirmed numerically in Fig. 3(b). A similar analysis yields  $f(x) \rightarrow -(c/3) \log(|x|)$ , again diverging logarithmically as  $x \rightarrow 0^+$ . This divergence implies that, unlike the SSA construction of Ref.[18] that results in c-theorem, no nontrivial constraint arises for RG flows between 1+1-D CFTs.

**Illustration 3: CMI of SWSSB.** We now test the monotonicity constraints by studying the transition between trivial and strong-to-weak spontaneously symmetry-breaking (SWSSB) states [74, 75]. This transition is tuned by subjecting a trivial product state  $|+\rangle^{L_x \times L_y}$  on a square lattice to the channel  $\mathcal{E}_{\langle i,j \rangle}[\cdot] = (1 - p)(\cdot) + p Z_i Z_j(\cdot) Z_i Z_j$  acting on all nearest-neighbor

pairs [74]. The universality class at the critical point is the random bond Ising model's (RBIM) Nishimori multicriticality [94], with  $p_c \approx 0.109$ . A brief review of the SWSSB phase and its transition is provided in Ref.[39].

We compute the CMI using the tensor-network approach of Ref. [95] (see also Refs [96, 97]). We fix the total system size to  $L_y = l = 16$  and  $L_x = \alpha l = 48$ , with open boundary conditions along both directions. Region  $B$  is taken to be slab of size  $l_B \times l$  with  $l_B < l$ . Fig. 4 shows the CMI versus  $p$  for several  $l_B$ . As in the TFIM, for small  $l_B$  the CMI near the UV fixed point  $p \approx p_c$  exceeds that at the two IR fixed points  $p = 0$  and  $p = 0.5$ ; in particular, it is larger than  $\log 2$ , which is the CMI at  $p = 0.5$ . For larger  $l_B$  and  $p$  close to  $p_c$ , we observe apparent violations of this bound, attributable to the limited system sizes accessible in our numerics, namely  $l = 16$  (recall that Eq.(2) holds only when  $l/l_B, l|p-p_c|^\nu \rightarrow \infty$ ). Nevertheless, monotonicity of the CMI in  $l_B$  (Eq.(1)) remains intact, as it does not rely on CMI being a scaling function of  $x$ . The inset shows the CMI as a function of  $x = (p - p_c)l_B^{1/\nu}$  with  $\nu = 1.5$  [98]. Data collapse is good for  $|x| \gtrsim 0.2$ , while deviations appear in the UV regime  $|x| \lesssim 0.2$ , again due to finite-size effects. Analytically, we expect that  $f(x) \sim \log(1/|x|)$  when  $|x| \ll 1$ , since the CMI maps to the disorder-averaged free energy of the RBIM along the Nishimori line, which contains universal logarithmic contributions [99]. Finally, to further demonstrate UV finiteness of CMI, and to minimize finite-size effects arising from additional length scales, we also studied a geometry where  $A$ ,  $B$ , and  $C$  are all  $l \times l$  boxes [39]. In this setup, CMI  $I(p, l)$  is well described by a scaling function  $f((p-p_c)l^{1/\nu})$  with  $\nu \approx 1.5$ , consistent with Ref. [98].

We conclude with a speculative remark. Although all our examples were derived from lattice models, it is rea-

sonable to anticipate that CMI monotonicity holds also for field theories corresponding to interacting *motile* particles, such as flocks [100–104]. Consider an equilibrium critical point  $E$  in  $2 + 1$ D that, upon breaking detailed-balance, becomes immediately unstable to a nonequilibrium fixed point  $N$  governing an order-disorder transition into a flocking phase  $O$  with spontaneous  $O(2)$  symmetry breaking. In two spatial dimensions, such true long-range order is forbidden for local Gibbs states (Mermin–Wagner–Hohenberg theorem [105, 106]), suggesting that  $O$ —and hence both  $N$  and  $E$ —has a divergent Markov length. Monotonicity of CMI would then imply that  $E$  cannot be a Gibbs state of any local Hamiltonian. This is consistent with controlled analyses of continuous flocking transitions [107, 108], where incompressibility, inducing long-ranged dipolar interactions, provides a mechanism to avoid inhomogeneity/phase separation seen close to criticality in compressible flocks [103, 109–113]. From this perspective, CMI monotonicity offers an information-theoretic rationale for why non-locality at an equilibrium UV critical point might facilitate nontrivial nonequilibrium fixed points in the IR. More broadly, our results and such considerations motivate scaling of CMI as a promising guiding principle for exploring nonequilibrium phase diagrams.

**Acknowledgments:** We thank John McGreevy for helpful discussions. T.G. is supported by the National Science Foundation under Grant No. DMR-2521369. We acknowledge the hospitality of Kavli Institute for Theoretical Physics (KITP) and thank the organizers of the KITP programs “Noise-robust Phases of Quantum Matter”, and “Learning the Fine Structure of Quantum Dynamics in Programmable Quantum Matter”. This research was supported in part by grant NSF PHY-2309135 to the KITP.

---

[1] A. B. Zamolodchikov, Irreversibility of the flux of the renormalization group in a 2d field theory, *Jetp Letters* **43**, 565 (1986).

[2] I. Affleck and A. W. W. Ludwig, Universal noninteger “ground-state degeneracy” in critical quantum systems, *Phys. Rev. Lett.* **67**, 161 (1991).

[3] D. Friedan and A. Konechny, Boundary entropy of one-dimensional quantum systems at low temperature, *Phys. Rev. Lett.* **93**, 030402 (2004).

[4] J. L. Cardy, Is there a c-theorem in four dimensions?, *Physics Letters B* **215**, 749 (1988).

[5] Z. Komargodski and A. Schwimmer, On renormalization group flows in four dimensions, *Journal of High Energy Physics* **2011**, 99 (2011).

[6] R. C. Myers and A. Sinha, Seeing a c-theorem with holography, *Phys. Rev. D* **82**, 046006 (2010).

[7] D. L. Jafferis, I. R. Klebanov, S. S. Pufu, and B. R. Safdi, Towards the f-theorem: $n = 2$  field theories on the three-sphere, *Journal of High Energy Physics* **2011**, 102 (2011).

[8] H. Casini and M. Huerta, Renormalization group run-

ning of the entanglement entropy of a circle, *Phys. Rev. D* **85**, 125016 (2012).

[9] R. A. Patil and A. W. Ludwig, Shannon entropy of the measurement record at measurement-dominated criticality and rg flow: A c-theorem for effective central charge and a g-theorem for effective boundary entropy, arXiv preprint arXiv:2507.07959 (2025).

[10] A. Zamolodchikov, Renormalization group and perturbation theory about fixed points in two-dimensional field theory, *Sov. J. Nucl. Phys.(Engl. Transl.);(United States)* **46** (1987).

[11] A. W. Ludwig and J. L. Cardy, Perturbative evaluation of the conformal anomaly at new critical points with applications to random systems, *Nuclear Physics B* **285**, 687 (1987).

[12] D. A. Huse, Exact exponents for infinitely many new multicritical points, *Phys. Rev. B* **30**, 3908 (1984).

[13] T. Appelquist, A. G. Cohen, and M. Schmaltz, A new constraint on strongly coupled field theories, *Physical Review D* **60**, 045003 (1999).

[14] D. Anselmi, D. Freedman, M. T. Grisaru, and A. Jo-

hansen, Non-perturbative formulas for central functions of supersymmetric gauge theories, Nuclear Physics B **526**, 543 (1998).

[15] M. A. Luty, J. Polchinski, and R. Rattazzi, The a-theorem and the asymptotics of 4d quantum field theory, Journal of High Energy Physics **2013**, 1 (2013).

[16] I. R. Klebanov, S. S. Pufu, and B. R. Safdi, F-theorem without supersymmetry, Journal of High Energy Physics **2011**, 1 (2011).

[17] T. Grover, Entanglement monotonicity and the stability of gauge theories in three spacetime dimensions, Physical review letters **112**, 151601 (2014).

[18] H. Casini and M. Huerta, A finite entanglement entropy and the c-theorem, Physics Letters B **600**, 142 (2004).

[19] H. Casini, I. S. Landea, and G. Torroba, The g-theorem and quantum information theory, Journal of High Energy Physics **2016**, 1 (2016).

[20] H. Casini, I. S. Landea, and G. Torroba, Irreversibility in quantum field theories with boundaries, Journal of High Energy Physics **2019**, 1 (2019).

[21] H. Casini, I. S. Landea, and G. Torroba, Entropic g theorem in general spacetime dimensions, Phys. Rev. Lett. **130**, 111603 (2023).

[22] J. Harper, H. Kanda, T. Takayanagi, and K. Tasuki, g theorem from strong subadditivity, Physical Review Letters **133**, 031501 (2024).

[23] T. Grover, Certain general constraints on the many-body localization transition, arXiv preprint arXiv:1405.1471 (2014).

[24] I. H. Kim, Long-range entanglement is necessary for a topological storage of quantum information, Phys. Rev. Lett. **111**, 080503 (2013).

[25] B. Shi, K. Kato, and I. H. Kim, Fusion rules from entanglement, Annals of Physics **418**, 168164 (2020).

[26] J.-L. Huang, J. McGreevy, and B. Shi, Knots and entanglement, SciPost Phys. **14**, 141 (2023).

[27] I. H. Kim, X. Li, T.-C. Lin, J. McGreevy, and B. Shi, Conformal geometry from entanglement, SciPost Phys. **18**, 102 (2025).

[28] T.-C. Lin and J. McGreevy, Conformal field theory ground states as critical points of an entropy function, Phys. Rev. Lett. **131**, 251602 (2023).

[29] X. Li, T.-C. Lin, and J. McGreevy, A systematic search for conformal field theories in very small spaces, arXiv preprint arXiv:2509.04596 (2025).

[30] T.-H. Yang, B. Shi, and J. Y. Lee, Topological mixed states: Axiomatic approaches and phases of matter, arXiv preprint arXiv:2506.04221 (2025).

[31] S. Sang and T. H. Hsieh, Stability of mixed-state quantum phases via finite markov length, Phys. Rev. Lett. **134**, 070403 (2025).

[32] S. Sang, L. A. Lessa, R. S. Mong, T. Grover, C. Wang, and T. H. Hsieh, Mixed-state phases from local reversibility, arXiv preprint arXiv:2507.02292 (2025).

[33] A. Coser and D. Pérez-García, Classification of phases for mixed states via fast dissipative evolution, Quantum **3**, 174 (2019).

[34] S. Sang, Y. Zou, and T. H. Hsieh, Mixed-state quantum phases: Renormalization and quantum error correction, Phys. Rev. X **14**, 031044 (2024).

[35] C.-F. Chen and C. Rouzé, Quantum gibbs states are locally markovian, arXiv preprint arXiv:2504.02208 (2025).

[36] P. Clifford and J. M. Hammersley, Markov fields on finite graphs and lattices (1971).

[37] M. S. Leifer and D. Poulin, Quantum graphical models and belief propagation, Annals of Physics **323**, 1899 (2008).

[38] W. Brown and D. Poulin, Quantum markov networks and commuting hamiltonians, arXiv preprint arXiv:1206.0755 (2012).

[39] See Supplemental Material for details.

[40] D. V. Fursaev, Entanglement entropy in critical phenomena and analog models of quantum gravity, Phys. Rev. D **73**, 124025 (2006).

[41] S. Ryu and T. Takayanagi, Aspects of holographic entanglement entropy, Journal of High Energy Physics **2006**, 045 (2006).

[42] S. N. Solodukhin, Entanglement entropy, conformal invariance and extrinsic geometry, Physics Letters B **665**, 305 (2008).

[43] M. A. Metlitski, C. A. Fuertes, and S. Sachdev, Entanglement entropy in the  $o(n)$  model, Phys. Rev. B **80**, 115122 (2009).

[44] T. Grover, A. M. Turner, and A. Vishwanath, Entanglement entropy of gapped phases and topological order in three dimensions, Phys. Rev. B **84**, 195120 (2011).

[45] H. Liu and M. Mezei, A refinement of entanglement entropy and the number of degrees of freedom, Journal of High Energy Physics **2013**, 1 (2013).

[46] H. Casini, M. Huerta, R. C. Myers, and A. Yale, Mutual information and the f-theorem, Journal of High Energy Physics **2015**, 1 (2015).

[47] M. Van Raamsdonk, Finite entropy sums in quantum field theory, arXiv preprint arXiv:2508.21276 (2025).

[48] A prototypical example is provided by a 1+1-D CFT with central charge  $c$ , where the divergent part of the entanglement entropy  $S_X$  for a region  $X$  consisting of  $N$  disjoint pieces is  $2N \times \frac{c}{6} \log(1/a)$ , reflecting the additive contribution from the  $2N$  entangling boundary points [50]. This expression remains true even when the CFT is slightly perturbed and acquires a finite correlation length  $\xi \gg a$ , precisely because these divergences arise from singularities localized at length scales much less than  $\xi$ .

[49] C. Holzhey, F. Larsen, and F. Wilczek, Geometric and renormalized entropy in conformal field theory, Nuclear Physics B **424**, 443 (1994).

[50] P. Calabrese and J. Cardy, Entanglement entropy and quantum field theory, Journal of Statistical Mechanics: Theory and Experiment **2004**, P06002 (2004).

[51] M. A. Levin and X.-G. Wen, String-net condensation: A physical mechanism for topological phases, Phys. Rev. B **71**, 045110 (2005).

[52] S. Vardhan, A. Y. Wei, and Y. Zou, Petz recovery from subsystems in conformal field theory, Journal of High Energy Physics **2024**, 1 (2024).

[53] V. Balasubramanian, N. Jokela, A. Pönni, and A. V. Ramallo, Information flows in strongly coupled abjm theory, Journal of High Energy Physics **2019**, 1 (2019).

[54] P. C. Martin, E. D. Siggia, and H. A. Rose, Statistical dynamics of classical systems, Phys. Rev. A **8**, 423 (1973).

[55] H.-K. Janssen, On a lagrangean for classical field dynamics and renormalization group calculations of dynamical critical properties, Zeitschrift für Physik B Condensed Matter **23**, 377 (1976).

[56] C. d. Dominicis, Techniques de renormalisation de la

théorie des champs et dynamique des phénomènes critiques, in *J. Phys., Colloq.*, Vol. 37 (1976) p. 247.

[57] U. C. Täuber, *Critical dynamics: A field theory approach to equilibrium and non-equilibrium scaling behavior* (Cambridge University Press, 2014).

[58] H. Ma, A. T. Schmitz, S. A. Parameswaran, M. Hermele, and R. M. Nandkishore, Topological entanglement entropy of fracton stabilizer codes, *Physical Review B* **97**, 125101 (2018).

[59] A. Paramekanti, L. Balents, and M. P. A. Fisher, Ring exchange, the exciton bose liquid, and bosonization in two dimensions, *Phys. Rev. B* **66**, 054526 (2002).

[60] C. Chamon, Quantum glassiness in strongly correlated clean systems: An example of topological overprotection, *Phys. Rev. Lett.* **94**, 040402 (2005).

[61] J. Haah, Local stabilizer codes in three dimensions without string logical operators, *Phys. Rev. A* **83**, 042330 (2011).

[62] S. Vijay, J. Haah, and L. Fu, Fracton topological order, generalized lattice gauge theory, and duality, *Phys. Rev. B* **94**, 235157 (2016).

[63] M. Pretko, Subdimensional particle structure of higher rank  $u(1)$  spin liquids, *Phys. Rev. B* **95**, 115139 (2017).

[64] P. Gorantla, H. T. Lam, N. Seiberg, and S.-H. Shao, Low-energy limit of some exotic lattice theories and uv/ir mixing, *Phys. Rev. B* **104**, 235116 (2021).

[65] N. Seiberg and S.-H. Shao, Exotic  $U(1)$  symmetries, duality, and fractons in 3+1-dimensional quantum field theory, *SciPost Phys.* **9**, 046 (2020).

[66] J. Haah, Bifurcation in entanglement renormalization group flow of a gapped spin model, *Physical Review B* **89**, 075119 (2014).

[67] W. Shirley, K. Slagle, and X. Chen, Foliated fracton order in the checkerboard model, *Physical Review B* **99**, 115123 (2019).

[68] A. Dua, P. Sarkar, D. J. Williamson, and M. Cheng, Bifurcating entanglement-renormalization group flows of fracton stabilizer models, *Physical Review Research* **2**, 033021 (2020).

[69] Y. F. Zhang and S. Gopalakrishnan, Stability of mixed-state phases under weak decoherence, arXiv preprint arXiv:2511.01976 (2025).

[70] M. Kardar, G. Parisi, and Y.-C. Zhang, Dynamic scaling of growing interfaces, *Physical Review Letters* **56**, 889 (1986).

[71] K. Bassler and B. Schmittmann, Critical dynamics of nonconserved ising-like systems, *Physical review letters* **73**, 3343 (1994).

[72] T. Hwa and M. Kardar, Dissipative transport in open systems: An investigation of self-organized criticality, *Physical review letters* **62**, 1813 (1989).

[73] T. Hwa and M. Kardar, Avalanches, hydrodynamics, and discharge events in models of sandpiles, *Physical Review A* **45**, 7002 (1992).

[74] J. Y. Lee, C.-M. Jian, and C. Xu, Quantum criticality under decoherence or weak measurement, *PRX Quantum* **4**, 030317 (2023).

[75] L. A. Lessa, R. Ma, J.-H. Zhang, Z. Bi, M. Cheng, and C. Wang, Strong-to-weak spontaneous symmetry breaking in mixed quantum states, arXiv preprint arXiv:2405.03639 (2024).

[76] F. Ginelli, V. Ahlers, R. Livi, D. Mukamel, A. Pikovsky, A. Politi, and A. Torcini, From multiplicative noise to directed percolation in wetting transitions, *Physical Review E* **68**, 065102 (2003).

[77] Y.-H. Chen and T. Grover, Local reversibility and divergent markov length in 1+ 1-d directed percolation, arXiv preprint arXiv:2512.07220 (2025).

[78] B. Zeng and D.-L. Zhou, Topological and error-correcting properties for symmetry-protected topological order, *Europhysics Letters* **113**, 56001 (2016).

[79] M. Levin and X.-G. Wen, Detecting topological order in a ground state wave function, *Phys. Rev. Lett.* **96**, 110405 (2006).

[80] A. Kitaev and J. Preskill, Topological entanglement entropy, *Physical review letters* **96**, 110404 (2006).

[81] H. Casini and M. Huerta, Entanglement entropy in free quantum field theory, *Journal of Physics A: Mathematical and Theoretical* **42**, 504007 (2009).

[82] P. Bueno, H. Casini, O. L. Andino, and J. Moreno, Disks globally maximize the entanglement entropy in 2+1 dimensions, *Journal of High Energy Physics* **2021**, 1 (2021).

[83] Here  $p$ -bounded noise means that, upon measuring  $\mathcal{E}[(\uparrow\downarrow\uparrow\downarrow)^{\otimes L}]$  in the computational basis, the marginal probability of observing an all-down configuration on any subregion  $X$  is bounded by  $p^{|X|}$ , where  $|X|$  denotes the size of  $X$ . An analogous statement holds for  $\mathcal{E}[(\downarrow\uparrow\downarrow\uparrow)^{\otimes L}]$ .

[84] Y. F. Zhang and S. Gopalakrishnan, Conditional mutual information and information-theoretic phases of decohered gibbs states, *Physical review letters* **135**, 160401 (2025).

[85] R. M. Fano and D. Hawkins, Transmission of information: A statistical theory of communications, *American Journal of Physics* **29**, 793 (1961).

[86] R. Fernández and A. Toom, Non-gibbsianness of the invariant measures of non-reversible cellular automata with totally asymmetric noise, arXiv preprint math-ph/0101014 (2001).

[87] J. Lebowitz and R. H. Schonmann, Pseudo-free energies and large deviations for non gibbsian fkg measures, *Probability theory and related fields* **77**, 49 (1988).

[88] We thank John McGreevy for a helpful discussion on this point.

[89] A. L. Toom, Nonergodic multidimensional system of automata, *Problemy Peredachi Informatsii* **10**, 70 (1974).

[90] A. L. Toom, Stable and attractive trajectories in multicomponent systems, in *Multicomponent Random Systems*, *Advances in Probability and Related Topics*, Vol. 6, edited by R. L. Dobrushin and Y. G. Sinai (Marcel Dekker, New York, 1980) pp. 549–575.

[91] The existence of a nonzero threshold shows that violating alignment suppression does not imply that  $\rho(p)$  is distinct from the classical SSB phase, and hence is not a universal characteristic of non-Gibbsianness.

[92] J. Lloyd, D. A. Abanin, and S. Gopalakrishnan, Diverging conditional correlation lengths in the approach to high temperature, arXiv preprint arXiv:2508.02567 (2025).

[93] P. Calabrese and J. Cardy, Entanglement entropy and quantum field theory, *Journal of statistical mechanics: theory and experiment* **2004**, P06002 (2004).

[94] H. Nishimori, Internal energy, specific heat and correlation function of the bond-random ising model, *Progress of Theoretical Physics* **66**, 1169 (1981).

[95] Y.-H. Chen and T. Grover, Zipping many-body quan-

tum states: a scalable approach to diagonal entropy, arXiv preprint arXiv:2502.18898 (2025), our code implementation is also publicly available at <https://github.com/yuhsuehchen/strong-to-weak-SSB-cmi>.

[96] G.-Y. Zhu, N. Tantivasadakarn, A. Vishwanath, S. Trebst, and R. Verresen, Nishimori's cat: Stable long-range entanglement from finite-depth unitaries and weak measurements, *Physical Review Letters* **131**, 200201 (2023).

[97] Z.-Q. Wan, X.-D. Dai, and G.-Y. Zhu, Revisiting nishimori multicriticality through the lens of information measures, arXiv preprint arXiv:2511.02907 (2025).

[98] F. Merz and J. Chalker, Two-dimensional random-bond ising model, free fermions, and the network model, *Physical Review B* **65**, 054425 (2002).

[99] J. L. Cardy and I. Peschel, Finite-size dependence of the free energy in two-dimensional critical systems, *Nuclear Physics B* **300**, 377 (1988).

[100] T. Vicsek, A. Czirók, E. Ben-Jacob, I. Cohen, and O. Shochet, Novel type of phase transition in a system of self-driven particles, *Physical review letters* **75**, 1226 (1995).

[101] J. Toner and Y. Tu, Long-range order in a two-dimensional dynamical XY model: How birds fly together, *Physical Review Letters* **75**, 4326 (1995).

[102] S. Ramaswamy, The mechanics and statistics of active matter, *Annu. Rev. Condens. Matter Phys.* **1**, 323 (2010).

[103] H. Chaté, Dry aligning dilute active matter, *Annual Review of Condensed Matter Physics* **11**, 189 (2020).

[104] J. Toner, The physics of flocking: birth, death, and flight in active matter, Cambridge University Press (2024).

[105] N. D. Mermin and H. Wagner, Absence of ferromagnetism or antiferromagnetism in one- or two-dimensional isotropic heisenberg models, *Phys. Rev. Lett.* **17**, 1133 (1966).

[106] P. C. Hohenberg, Existence of long-range order in one and two dimensions, *Phys. Rev.* **158**, 383 (1967).

[107] L. Chen, J. Toner, and C. F. Lee, Critical phenomenon of the order-disorder transition in incompressible active fluids, *New Journal of Physics* **17** (2015).

[108] L. Chen, C. F. Lee, and J. Toner, Mapping two-dimensional polar active fluids to two-dimensional soap and one-dimensional sandblasting, *Nature communications* **7**, 12215 (2016).

[109] E. Bertin, M. Drouz, and G. Grégoire, Boltzmann and hydrodynamic description for self-propelled particles, *Phys. Rev. E* **74**, 022101 (2006).

[110] S. Mishra, A. Baskaran, and M. C. Marchetti, Fluctuations and pattern formation in self-propelled particles, *Phys. Rev. E* **81**, 061916 (2010).

[111] F. D. C. Farrell, M. C. Marchetti, D. Marenduzzo, and J. Tailleur, Pattern formation in self-propelled particles with density-dependent motility, *Phys. Rev. Lett.* **108**, 248101 (2012).

[112] S. Yamanaka and T. Ohta, Formation and collision of traveling bands in interacting deformable self-propelled particles, *Phys. Rev. E* **89**, 012918 (2014).

[113] J. Bialké, H. Löwen, and T. Speck, Microscopic theory for the phase separation of self-propelled repulsive disks, *Europhysics Letters* **103**, 30008 (2013).

[114] F. J. MacWilliams and N. J. A. Sloane, *The theory of error-correcting codes*, Vol. 16 (Elsevier, 1977).

[115] C. de Groot, A. Turzillo, and N. Schuch, Symmetry Protected Topological Order in Open Quantum Systems, *Quantum* **6**, 856 (2022).

[116] R. Ma and C. Wang, Average symmetry-protected topological phases, *Phys. Rev. X* **13**, 031016 (2023).

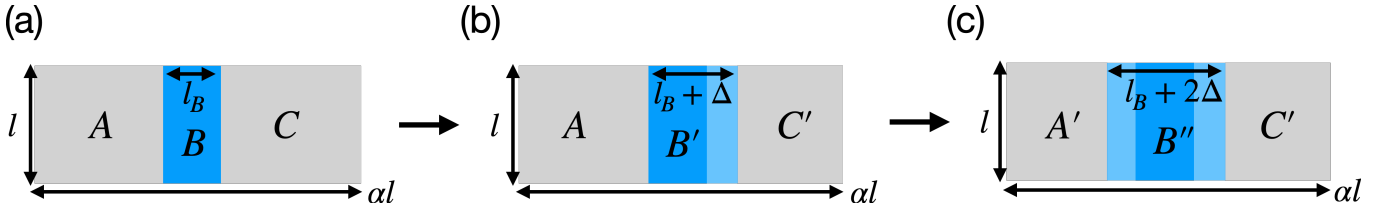


FIG. 5. To prove that  $I(A : C|B) \geq I(A' : C'|B'')$ , we first introduce an intermediate configuration  $AB'C'$  in (b) that interpolates between  $ABC$  in (a) and  $A'B''C'$  in (c), and then establish the chain of inequalities  $I(A : C|B) \geq I(A : C'|B') \geq I(A' : C'|B'')$ .

## Appendix A: Proofs of constraints on CMI using SSA

### 1. Proof of Eq.(1) in the main text

We now show that  $I(l|l_B) \equiv I(A : C|B) \geq I(l|l_B + 2\Delta) \equiv I(A' : C'|B'')$ , for all  $\Delta > 0$  [see Fig. 5(a) and (c)], which corresponds to Eq. (1) in the main text. It is conceptually convenient to introduce an intermediate configuration  $AB'C'$  [Fig. 5(b)] that interpolates between  $ABC$  and  $A'B''C'$ . In particular, we establish the chain of inequalities  $I(A : C|B) \geq I(A : C'|B') \geq I(A' : C'|B'')$ .

Let us define  $\delta \equiv B' \setminus B$ , so that  $B' = B\delta$  and  $C' = C \setminus \delta$ . The key observation underlying  $I(A : C|B) \geq I(A : C'|B')$  is that  $B'C' = BC$ , which implies  $I(A : C'|B') = S(AB') + S(B'C') - S(B') - S(AB'C') = S(AB\delta) + S(BC) - S(B\delta) - S(ABC)$ . Therefore,

$$\begin{aligned} I(A : C'|B') - I(A : C|B) &= [S(AB\delta) + S(BC) - S(B\delta) - S(ABC)] - [S(AB) + S(BC) - S(B) - S(ABC)] \\ &= -[S(AB) + S(B\delta) - S(B) - S(AB\delta)] \\ &= -I(A : \delta|B) \leq 0, \end{aligned} \quad (\text{A1})$$

where the final inequality follows from SSA. The same calculation shows that  $I(A : C'|B') \geq I(A' : C'|B'')$ , and hence  $I(A : C|B) \geq I(A' : C'|B'')$ .

### Proof of Eq.(3) in the main text

It is illuminating to first rewrite Eq. (3) in the main text solely in terms of the classical-quantum state  $\sigma = \sum_\alpha p_\alpha |\alpha\rangle\langle\alpha|_D \otimes \rho_\alpha$ . Clearly,  $I_\sigma(A : C|B) = I_\rho(A : C|B)$  and  $\sum_\alpha p_\alpha I_{\rho_\alpha}(A : C|B) = I_\sigma(A : C|B, D)$ . Eq. (3) is therefore equivalent to

$$I_\sigma(A : C|B) \leq I_\sigma(A : C|B, D) + S_\sigma(D|B). \quad (\text{A2})$$

Since all quantities are now expressed in terms of  $\sigma$ , we will omit the subscript in  $I$  and  $S$  in the following for notational simplicity.

A straightforward use of the definition of CMI shows that

$$\begin{aligned} I(A : C|B) - I(A : C|B, D) &= [S(AB) + S(BC) - S(B) - S(ABC)] - [S(ABD) + S(BCD) - S(BD) - S(ABCD)] \\ &= [(S(BD) - S(B)) - (S(ABD) - S(AB))] - [S(ABC) + S(BCD) - S(BC) - S(ABCD)] \\ &= [S(D|B) - S(D|AB)] - I(A : D|BC) \\ &\leq S(D|B) - S(D|AB), \end{aligned} \quad (\text{A3})$$

where we have used the strong subadditivity in the final line. Eq.(A3) is fairly general for any quadripartition  $A, B, C, D$ . Now, using the fact that  $\sigma = \sum_\alpha p_\alpha |\alpha\rangle\langle\alpha|_D \otimes \rho_\alpha$  and thus  $D$  is only classically correlated with the rest of the system, one has  $S(D|X) \geq 0$  for any  $X \in ABC$ . Choosing  $X = AB$ , one then has  $S(D|B) - S(D|AB) \leq S(D|B)$ , and thus the desired inequality Eq.(A2) holds.

## Appendix B: Proof that $S(D|B)$ is exponentially small in $N_B$

As discussed in the main text, the CMI of  $\rho$  can be bounded using a convex decomposition  $\rho = \sum_{\alpha} p_{\alpha} \rho_{\alpha}$  as  $I_{\rho}(A : C|B) \leq \sum_{\alpha} p_{\alpha} I_{\rho_{\alpha}}(A : C|B) + S_{\sigma}(D|B)$ , where  $\sigma = \sum_{\alpha} p_{\alpha} |\alpha\rangle\langle\alpha|_D \otimes \rho_{\alpha}$ . Therefore, showing that both  $S_{\sigma}(D|B)$  and each  $I_{\rho_{\alpha}}(A : C|B)$  decay exponentially with  $l_B$  is sufficient to establish that  $I_{\rho}(A : C|B)$  decays exponentially. For the classical SSB discussed in the main text,  $\rho = \frac{1}{2} \mathcal{E}[(|\uparrow\rangle\langle\uparrow|)^{\otimes N}] + \frac{1}{2} \mathcal{E}[(|\downarrow\rangle\langle\downarrow|)^{\otimes N}]$  and thus

$$\sigma = \frac{1}{2} |\alpha = \uparrow\rangle\langle\alpha = \uparrow|_D \otimes \mathcal{E}[(|\uparrow\rangle\langle\uparrow|)^{\otimes N}] + \frac{1}{2} |\alpha = \downarrow\rangle\langle\alpha = \downarrow|_D \otimes \mathcal{E}[(|\downarrow\rangle\langle\downarrow|)^{\otimes N}]. \quad (\text{B1})$$

The goal of this appendix is to show that for any  $p$ -bounded channel there exists a threshold  $p_c$  such that, for all  $p < p_c$ ,  $S_{\sigma}(D|B)$  decays exponentially as a function of  $l_B$ . Here  $p$ -bounded noise means that, upon measuring  $\mathcal{E}[(|\uparrow\rangle\langle\uparrow|)^{\otimes N}]$  in the computational basis, the marginal probability of observing an all-down configuration on any subregion  $X$  is bounded by  $p^{|X|}$ , where  $|X|$  denotes the size of  $X$ . An analogous statement holds for  $\mathcal{E}[(|\downarrow\rangle\langle\downarrow|)^{\otimes N}]$ .

To show that  $S_{\sigma}(D|B)$  decays exponentially, we perform a measurement of all qubits in  $B$  in the computational basis, which results in a classical bitstring  $Y$ . This is a quantum channel acting on  $B$  and data processing combined with Fano's inequality implies  $S_{\sigma}(D|B) \leq S(D|Y) = H_2(P_{\text{decoder}})$ , where  $D$  and  $Y$  are now both classical variables,  $H_2(x) = -(1-x)\ln(1-x) - x\ln x$  is the binary entropy, and  $P_{\text{decoder}}$  is the decoding error probability for a chosen decoder. It is well known that for sufficiently small  $p$ ,  $P_{\text{decoder}} \leq e^{-|B|/\epsilon}$  for the majority-vote decoder. We derive this bound below for completeness.

The majority-vote decoder on  $Y$  proceeds by mapping configurations  $\{z_j\}$  satisfying  $\sum_{j=1}^{N_B} z_j > 0$  ( $\sum_{j=1}^{N_B} z_j \leq 0$ ) to the outcome  $m = \uparrow$  ( $\downarrow$ ), where  $N_B$  denotes the size of region  $B$ . For the geometry considered in the main text,  $N_B \propto l_B$ , and hence exponential decay in  $N_B$  implies exponential decay in  $l_B$ . The decoding error probability is  $P_{\text{decoder}} = [\Pr(m = \downarrow | \alpha = \uparrow) + \Pr(m = \uparrow | \alpha = \downarrow)]/2$ . Now, using the  $p$ -bounded noise assumption, we obtain

$$\Pr(m = \downarrow | d = \uparrow) \leq \sum_{k=N_B/2}^{N_B} \binom{N_B}{k} p^k. \quad (\text{B2})$$

For  $p < 1$ , one has  $p^k \leq p^{N_B/2}$  for all  $k \geq N_B/2$ , which gives

$$\sum_{k=N_B/2}^{N_B} \binom{N_B}{k} p^k \leq p^{N_B/2} \sum_{k=N_B/2}^{N_B} \binom{N_B}{k} \leq p^{N_B/2} 2^{N_B}. \quad (\text{B3})$$

It follows that  $\Pr(m = \downarrow | d = \uparrow) \leq (4p)^{N_B/2}$ . An identical bound holds for  $\Pr(m = \uparrow | d = \downarrow)$ . Therefore, for  $p < 1/4$ , the decoding error probability satisfies  $P_{\text{decoder}} \leq (4p)^{N_B/2}$  and decays exponentially with  $N_B$ . Using the inequality  $H_2(x) \leq x[1 - \ln x]$ , we conclude that  $H_2(P_{\text{decoder}})$ , and hence  $S_{\sigma}(D|B)$ , decays exponentially as a function of  $N_B$ , and thus as a function of  $l_B$ .

This discussion generalizes to any classical  $(n, k, d)$  code, with the restriction that the same type of code can also be defined for the reduced system  $B$  with code parameters  $(N_B, k_B, d_B)$ . An example is first-order Reed-Muller code where an  $(n = 2^m, k = m+1, d = 2^{m-1})$  code can be ‘punctured’ to obtain an  $(n' = n/2, k' = k-1, d' = d/2)$  code [114]. We again measure all qubits in  $B$ , resulting in a classical bitstring  $Y$ . For a fixed transmitted message  $D = i$  (where  $i = 1, 2, \dots, k_B$ ), the codeword on  $B$  is  $c_d$ , then let's denote the number of flipped bits in  $B$  relative to the transmitted codeword as  $|E|$ . By the defining property of the code distance  $d_B$ , if  $|E| \leq (d_B - 1)/2$ , decoding succeeds. Therefore, the decoding error is  $\Pr(|E| \geq (d_B - 1)/2 | D = i) \leq \sum_{j=1}^{N_B} \binom{N_B}{j} p^j$ . Using the same series of inequalities as for the repetition code, one finds  $\Pr(|E| \geq (d_B - 1)/2 | D = i) \leq 2^{N_B} p^{d_B/2}$ , which decays exponentially with  $N_B$  as long as  $p < 2^{-2N_B/d_B}$  (note that we recover the bound  $p_c = 1/4$  for the repetition code where  $d_B = N_B$ ).

## Appendix C: Conditional mutual information of classical SSB under decoherence

The goal of this appendix is to analytically study the CMI of the one-dimensional mixed state

$$\rho_L(p, q) = \frac{1}{2} [(1-q)|\uparrow\rangle\langle\uparrow| + q|\downarrow\rangle\langle\downarrow|]^l + \frac{1}{2} [(1-p)|\downarrow\rangle\langle\downarrow| + p|\uparrow\rangle\langle\uparrow|]^l, \quad (\text{C1})$$

which can be obtained by subjecting a classical SSB state  $\rho_0 = \frac{1}{2}(|\uparrow\rangle\langle\uparrow|)^l + \frac{1}{2}(|\downarrow\rangle\langle\downarrow|)^l$  to a product of single-site channels that flip a  $\downarrow$  spin with probability  $p$  and an  $\uparrow$  spin with probability  $q$ . A useful property of  $\rho_l$  that dramatically

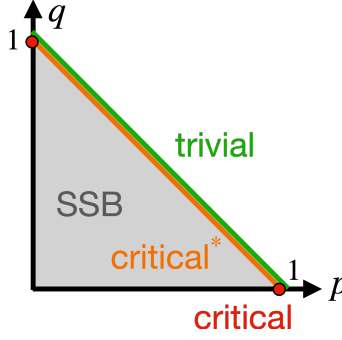


FIG. 6. Phase diagram of the mixed state in Eq.(C1). The  $q = 0$  line corresponds to the case studied in the main text. Interestingly, the correlation-length exponent along the  $q = 0$  line (corresponding to the case studied in the main text) and along the  $p = 0$  line is  $\nu = 1$ . This differs from the exponent  $\nu = 2$  obtained when  $p, q \neq 0$ . We denote the former case as “critical” while the latter case as “critical\*”.

simplifies the calculation of the CMI is that the reduced density matrix  $\rho_X \equiv \text{tr}_{\bar{X}} \rho_l$  of any region  $X$  of size  $|X|$  takes the same form as Eq. (C1), namely  $\rho_X = \rho_{|X|} = \frac{1}{2}[(1-q)|\uparrow\rangle\langle\uparrow| + q|\downarrow\rangle\langle\downarrow|]^{[X]} + \frac{1}{2}[(1-p)|\downarrow\rangle\langle\downarrow| + p|\uparrow\rangle\langle\uparrow|]^{[X]}$ . Therefore, the CMI  $I(A : C|B)$  of total system size  $\bar{l} = l_B + 2r$  and  $B$  of size  $l_B$  takes the form

$$I(\bar{l} = l_B + 2r|l_B) = I(r, l_B) = S(AB) + S(BC) - S(B) - S(ABC) = 2H_{r+l_B} - H_{l_B} - H_{l_B+2r}, \quad (\text{C2})$$

where  $H_r = H_r(p, q)$  denotes the Shannon entropy of the reduced density matrix  $\rho_r(p, q)$  and is given by

$$H_r(p, q) = - \sum_{m=0}^r \binom{r}{m} t_{r,m} \log t_{r,m}, \quad t_{r,m} = \frac{1}{2}[(1-q)^{r-m} q^m + p^{r-m} (1-p)^m]. \quad (\text{C3})$$

In the following, we show that the CMI becomes singular in the limit  $\epsilon = p + q - 1 \rightarrow 0^-$ , which underlies the phase diagram shown in Fig. 6. Interestingly, the correlation-length exponent along the  $q = 0$  line (corresponding to the case studied in the main text) and along the  $p = 0$  line is  $\nu = 1$ , which differs from the exponent  $\nu = 2$  obtained when  $p, q \neq 0$ . We note that, unlike the  $q = 0$  and  $p = 0$  lines, the case  $p, q \neq 0$  does not violate the alignment-suppression property discussed in the main text. We first analyze the  $q = 0$  case and then turn to the case with  $p, q \neq 0$ .

### CMI along the $q = 0$ line

Along the  $q = 0$  line, the probability  $t_{r,m}$  takes a simpler form

$$t_{r,m} = \frac{\delta_{m,0} + p^{r-m} (1-p)^m}{2} = \begin{cases} \frac{1+p^r}{2}, & m = 0, \\ \frac{p^{r-m} (1-p)^m}{2}, & m \geq 1. \end{cases} \quad (\text{C4})$$

It follows that

$$\begin{aligned} H_r &= -\frac{1+p^r}{2} \log\left(\frac{1+p^r}{2}\right) - \sum_{m=1}^r \binom{r}{m} \frac{p^{r-m} (1-p)^m}{2} \log\left(\frac{p^{r-m} (1-p)^m}{2}\right) \\ &= -\frac{1+p^r}{2} \log\left(\frac{1+p^r}{2}\right) - \sum_{m=0}^r \binom{r}{m} \frac{p^{r-m} (1-p)^m}{2} \log\left(\frac{p^{r-m} (1-p)^m}{2}\right) + \frac{p^r}{2} \log(p^r) \\ &= \log 2 + \frac{r}{2} h(p) - \left(\frac{1}{2}(1+p^r) \log(1+p^r) - \frac{1}{2} p^r \log(p^r)\right) \\ &= \log 2 + \frac{r}{2} h(p) - g(r) \end{aligned} \quad (\text{C5})$$

where  $h(p) = -p \log(p) - (1-p) \log(1-p)$  is the binary entropy and we denote  $g(r) = \frac{1}{2}(1+p^r) \log(1+p^r) - \frac{1}{2} p^r \log(p^r)$ . In the third line, we have used the properties that  $\sum_{m=0}^r \binom{r}{m} p^{r-m} (1-p)^m = 1$  and  $\sum_{m=0}^r \binom{r}{m} p^{r-m} (1-p)^m \log(p^{r-m} (1-p)^m) = r h(p)$ .

Since the constant and linear terms cancel out when computing the CMI [Eq.(C2)], one finds

$$I(l_B + 2r|l_B, p) = g(l_B, p) + g(l_B + 2r, p) - 2g(l_B + r, p). \quad (\text{C6})$$

$$r = \infty$$

Let's first consider  $r \rightarrow \infty$  limit. Since  $\lim_{r \rightarrow \infty} g(r, p) = 0, \forall p < 1$ , Eq.(C6) simplifies to  $I(\infty|l_B, p) = g(l_B, p)$ . Now, in the limit  $l_B \rightarrow \infty$  and  $\epsilon = p - 1 \rightarrow 0^-$  with  $x \equiv l_B \epsilon$  finite, one can write  $p^{l_B} = e^{l_B \ln p} \approx e^{l_B \epsilon} = e^x$ . It follows that,

$$I(\infty|l_B, p) = g(l_B, p) = g(x) = \frac{1}{2}[(1 + e^x) \log(1 + e^x) - xe^x], \quad (\text{C7})$$

and thus we've derived Eq.(5) in the main text.

$$r < \infty$$

As in the previous case, in the limit  $l_B \rightarrow \infty$  and  $\epsilon = p - 1 \rightarrow 0^-$  with  $x \equiv l_B \epsilon$  finite, one can write  $p^{l_B} = e^{l_B \ln p} \approx e^{l_B \epsilon} = e^x$ . Furthermore, since now  $r$  is finite, one should treat  $\delta = xr/l_B$  as a small parameter in the  $l_B \rightarrow \infty$  limit. This implies  $p^{l_B+r} = e^{(l_B+r) \ln p} \approx e^{l_B \epsilon(1+r/l_B)} = e^{x+\delta}$ , and similarly  $p^{l_B+2r} = e^{x+2\delta}$ . It follows that

$$I(r, l_B, p) = g(x) + g(x + 2\delta) - 2g(x + \delta) = \delta^2 \partial_x^2 g = \delta^2 \left( \frac{1}{2} e^x \left[ \log(1 + e^{-x}) - \frac{1}{1 + e^x} \right] \right). \quad (\text{C8})$$

Substituting  $\delta = xr/l_B$ , one finds

$$I(r, l_B, p) = \left( \frac{r}{l_B} \right)^2 \left( \frac{x^2}{2} e^x \left[ \log(1 + e^{-x}) - \frac{1}{1 + e^x} \right] \right) = \left( \frac{r}{l_B} \right)^2 f[(p-1)l_B]. \quad (\text{C9})$$

Therefore, one finds the anomalous dimension  $\eta = 2$ .

### CMI for the $p, q \neq 0$ case

We now consider the CMI for the  $p, q \neq 0$  case. Let's first simplify the notation in Eq.(C3) by denoting  $A_m = (1-q)^{r-m}q^m$ ,  $B_m = p^{r-m}(1-p)^m$ , so that  $t_{r,m} = (A_m + B_m)/2 = A_m(1 + e^{-r\Delta_m})/2$  with

$$e^{-r\Delta_m} = \frac{B_m}{A_m} = \left( \frac{p}{1-q} \right)^{r-m} \left( \frac{1-p}{q} \right)^m = \exp \left( -r \left[ \left( 1 - \frac{m}{r} \right) \log \left( \frac{1-q}{p} \right) + \frac{m}{r} \log \left( \frac{q}{1-p} \right) \right] \right) \quad (\text{C10})$$

Similarly, we write

$$P_q^{(r)}(m) = \binom{r}{m} (1-q)^{r-m} q^m, \quad P_{1-p}^{(r)}(m) = \binom{r}{m} p^{r-m} (1-p)^m. \quad (\text{C11})$$

One can then rewrite Eq.(C3) as

$$\begin{aligned} H_r &= -\frac{1}{2} \sum_m P_q^{(r)}(m) \left( \log A_m - \log 2 + \log(1 + R_m) \right) - \frac{1}{2} \sum_m P_{1-p}^{(r)}(m) \left( \log B_m - \log 2 + \log(1 + R_m^{-1}) \right) \\ &= \log 2 + \frac{r}{2} [h(q) + h(p)] - \frac{1}{2} \mathcal{S}_{q \rightarrow p}(r) - \frac{1}{2} \mathcal{S}_{p \rightarrow q}(r), \end{aligned} \quad (\text{C12})$$

where

$$\mathcal{S}_{q \rightarrow p}(r) = \sum_m P_q^{(r)}(m) [\log(1 + e^{-r\Delta_m})], \quad \mathcal{S}_{p \rightarrow q}(r) = \sum_m P_{1-p}^{(r)}(m) [\log(1 + e^{r\Delta_m})]. \quad (\text{C13})$$

Since the constant and linear term cancel out when computing the CMI [Eq.(C2)], one finds

$$I(l = l_B + 2r | l_B, p, q) = \frac{1}{2} \left( [\mathcal{S}_{q \rightarrow p}(l_B) + \mathcal{S}_{p \rightarrow q}(l_B)] + [\mathcal{S}_{q \rightarrow p}(l_B + 2r) + \mathcal{S}_{p \rightarrow q}(l_B + 2r)] - 2[\mathcal{S}_{q \rightarrow p}(l_B + r) + \mathcal{S}_{p \rightarrow q}(l_B + r)] \right). \quad (\text{C14})$$

$$r = \infty$$

Similar to the  $q = 0$  case, when  $r = \infty$ , all the terms involving  $r$  vanishes, and thus one has

$$I(\infty | l_B, p, q) = \frac{1}{2} [\mathcal{S}_{q \rightarrow p}(l_B) + \mathcal{S}_{p \rightarrow q}(l_B)]. \quad (\text{C15})$$

We now consider the large- $l_B$ , small- $|\epsilon|$  limit of  $\mathcal{S}_{q \rightarrow p}(l_B)$ , where  $\epsilon = p + q - 1$  ( $\mathcal{S}_{q \rightarrow p}(l_B)$  can be obtained by exchanging  $q \leftrightarrow 1 - p$  and thus will be the same as  $\mathcal{S}_{q \rightarrow p}(l_B)$ ; this is because in the small- $|\epsilon|$  limit, one has  $q \approx 1 - p$ ). It's more convenient to introduce the variable  $u = m/l_B \in [0, 1]$  so that

$$\begin{aligned} \sum_m &\approx l_B \int_0^1 du, \quad P_q^{(l_B)}(m) \approx \frac{1}{\sqrt{2\pi l_B \sigma^2}} e^{-l_B \frac{(u-q)^2}{2\sigma^2}}, \quad \sigma^2 = q(1-q) \\ \Delta_m &= \Delta(u) = (1-u) \log\left(\frac{1-q}{p}\right) + u \log\left(\frac{q}{1-p}\right). \end{aligned} \quad (\text{C16})$$

We note that since  $p, q \neq 0$ ,  $\sigma^2$  is an order-one number. It follows that

$$\begin{aligned} \mathcal{S}_{q \rightarrow p}(l_B) &\approx \frac{\sqrt{l_B}}{\sqrt{2\pi\sigma^2}} \int_0^1 du e^{-l_B \frac{(u-q)^2}{2\sigma^2}} \log\left(1 + e^{-l_B \Delta(u)}\right) \\ &= \frac{\sqrt{l_B}}{\sqrt{2\pi\sigma^2}} \int_{-q}^{1-q} du e^{-l_B \frac{u^2}{2\sigma^2}} \log\left(1 + e^{-l_B \Delta(u+q)}\right) \\ &= \frac{1}{\sqrt{2\pi}} \int_{-\infty}^{\infty} dv e^{-\frac{v^2}{2}} \log\left(1 + e^{-l_B \Delta\left(\frac{\sigma v}{\sqrt{l_B}} + q\right)}\right), \end{aligned} \quad (\text{C17})$$

where in the last equality we let  $v = \sqrt{l_B}u/\sigma$  so that the end points of the integral go to  $\pm\infty$  in the larger- $l_B$  limit. Now, using  $p = (1-q) + \epsilon$  and  $1-p = q - \epsilon$  with  $\epsilon \rightarrow 0^-$  to expand  $l_B \Delta\left(\frac{\sigma v}{\sqrt{l_B}} + q\right)$  to  $\mathcal{O}(\epsilon^2)$ , one finds

$$l_B \Delta\left(\frac{\sigma v}{\sqrt{l_B}} + q\right) = v \frac{\sqrt{l_B} \epsilon}{\sigma} + \frac{1}{2} \left(\frac{\sqrt{l_B} \epsilon}{\sigma}\right)^2 + \mathcal{O}(\epsilon^3). \quad (\text{C18})$$

From Eq.(C18), it is obvious that the natural scaling variable is  $x = \epsilon \sqrt{l_B}/\sigma$ , and thus the correlation length exponent  $\nu = 2$ . Using  $\mathcal{S}_{q \rightarrow p}(l_B) = \mathcal{S}_{p \rightarrow q}(l_B)$  in the small- $|\epsilon|$  limit, one then has

$$I(\infty | l_B, p, q) = \mathcal{S}_{q \rightarrow p}(l_B) \approx \frac{1}{\sqrt{2\pi}} \int_{-\infty}^{\infty} dv e^{-\frac{v^2}{2}} \log\left(1 + e^{-\frac{x^2}{2} - vx}\right) \equiv \Phi(x). \quad (\text{C19})$$

$$r < \infty$$

Similar to the  $q = 0$  line, in the large- $l_B$ , small- $|\epsilon|$  limit, one has  $\epsilon \sqrt{l_B + r}/\sigma \approx x + \delta$  and  $\epsilon \sqrt{l_B + 2r}/\sigma \approx x + 2\delta$  with  $2\delta = xr/l_B$ . It follows that

$$I(l = l_B + 2r | l_B, p, q) = \delta^2 \Phi''(x) = \left(\frac{r}{l_B}\right)^2 \left[\frac{x^2}{4} \Phi''(x)\right] = \left(\frac{r}{l_B}\right)^2 f(x) \quad (\text{C20})$$

Therefore, one finds the anomalous dimension  $\eta = 2$ .

## Appendix D: A brief introduction to SWSSB

The goal of this appendix is to provide a brief review of the strong-to-weak spontaneously symmetry-breaking (SWSSB) phase (See Refs.[74, 75] for details). A density matrix is said to have a *strong symmetry* if  $U\rho = e^{i\theta}\rho$ , and a *weak symmetry* if  $U\rho U^\dagger = \rho$ , where  $U$  is the generator of the symmetry [115, 116]. Physically, a strong symmetry is a property of individual states, whereas a weak symmetry holds only at the level of the ensemble in general.

In the main paper we focus on examples where the relevant symmetry is generated by  $U = \prod_{j=1}^N X_j$  where  $N$  is the total system size. In this setting, a mixed state  $\rho$  is said to be an SWSSB state if the following three conditions are simultaneously satisfied [75]:

1. it is strongly symmetric;
2. there is no long-range order in the two-point correlation function, i.e.,  $\lim_{|i-j| \rightarrow \infty} \text{tr}(\rho Z_i Z_j) = 0$ ;
3. the fidelity between  $\rho$  and  $Z_i Z_j \rho Z_i Z_j$  saturates to a finite constant as  $|i - j| \rightarrow \infty$ , i.e.,  $\lim_{|i-j| \rightarrow \infty} F(\rho, Z_i Z_j \rho Z_i Z_j) = c > 0$ , where  $F(\rho, \sigma) = \text{tr}(\sqrt{\sqrt{\rho} \sigma \sqrt{\rho}})$ .

Either of the first or the second condition excludes the weakly symmetric, classical SSB state  $\rho_{\text{classical}} = \frac{1}{2}(|\uparrow\rangle\langle\uparrow|)^N + \frac{1}{2}(|\downarrow\rangle\langle\downarrow|)^N$ , while the second condition excludes the strongly symmetric, quantum SSB fixed point  $\rho_{\text{GHZ}} = |\text{GHZ}\rangle\langle\text{GHZ}|$ , where  $|\text{GHZ}\rangle = (|\uparrow\cdots\uparrow\rangle + |\downarrow\cdots\downarrow\rangle)/\sqrt{2}$ . The state  $\rho_{\text{classical}}$  exhibits nonvanishing two-point correlations and a non-trivial fidelity correlator, and therefore breaks the weak symmetry to nothing. On the other hand, the state  $\rho_{\text{GHZ}}$  also exhibits both nonvanishing two-point correlations and a nontrivial fidelity correlator, and can therefore be viewed as spontaneously breaking the strong symmetry to nothing.

By contrast, the SWSSB fixed point takes the form  $\rho_{\text{SWSSB}} = (I + U)/2^N$ , which can be interpreted as a maximally mixed state projected onto the global  $\mathbb{Z}_2$  charge-even sector. Since  $Z_i Z_j \rho_{\text{SWSSB}} Z_i Z_j = \rho_{\text{SWSSB}}$  for all  $i, j$ , one has  $F(\rho_{\text{SWSSB}}, Z_i Z_j \rho_{\text{SWSSB}} Z_i Z_j) = 1$ . We further note that  $\rho_{\text{SWSSB}}$  has CMI  $\log 2$ , since the entropy of any subsystem  $X$  of size  $|X|$  is  $S_X = |X| \log 2$ , while the entropy of the full system is  $S = (N - 1) \log 2$ . Physically, this nontrivial CMI originates from the global constraint and local irrecoverability [75].

A well-known transition between a trivial state and the SWSSB state is realized by subjecting a symmetric product state  $(|+\rangle\langle+|)^{L_x L_y}$  on a square lattice to the channel  $\mathcal{E}_{\langle i,j \rangle}[\cdot] = (1 - p)(\cdot) + p Z_i Z_j (\cdot) Z_i Z_j$  acting on all nearest-neighbor pairs [74]. In this setting, the mixed state is always diagonal in the Pauli- $X$  basis and can be written as  $\rho(p) \propto \sum_{x_j \text{ s.t. } \prod_j x_j = 1} \mathcal{Z}_{x_j}(p) |x_j\rangle\langle x_j|$ , where  $|x_j\rangle = |x_1, \dots, x_{L_x L_y}\rangle$ ,  $x_j = \pm 1$  denotes a product state in the Pauli- $X$  basis. The weight  $\mathcal{Z}_{x_j}(p) = \sum_{\{s_i\}} e^{\beta \sum_{\langle i,j \rangle} J_{\langle i,j \rangle} s_i s_j}$ , with  $\tanh \beta = 1 - 2p$ , is the partition function of the random-bond Ising model defined on the dual lattice  $\{\tilde{i}\}$ . Here the bond configuration  $\{J_{\langle i,j \rangle}\}$  is constrained to satisfy  $\prod_{\langle i,j \rangle \in j} J_{\langle i,j \rangle} = x_j$ . We emphasize that  $\rho(p)$  is generally not a Gibbs state of a local Hamiltonian, due to the summation  $\sum_{\{s_i\}}$  appearing in the weight  $\mathcal{Z}_{x_j}(p)$ . A straightforward calculation shows that the fidelity correlator is related to the free-energy cost of the random-bond Ising model along the Nishimori line, which is nonvanishing only for  $p > p_c \approx 0.109$  [94]. Consequently, the universality class of this transition is that of the random-bond Ising model's Nishimori multicriticality.

## Appendix E: Additional data for CMI of SWSSB

The goal of this appendix is to provide additional numerical evidence that the CMI of the SWSSB transition discussed in the main text is UV finite. To minimize finite-size effects arising from additional length scales, we consider the geometry shown in Fig. 7(a), where regions  $A$ ,  $B$ , and  $C$  are all  $l \times l$  boxes. Fig. 7(b) shows the CMI as a function of  $p$  for various values of  $l$ . We note that, unlike the geometry considered in the main text where the CMI decreases monotonically with increasing size of region  $B$ , no such monotonicity constraint exists in the present geometry. Fig. 7(c) shows a data collapse using the scaling ansatz  $I = f[(p - p_c)l^{1/\nu}]$  with  $p_c \approx 0.109$  and  $\nu = 1.5$ , confirming that the CMI is UV finite.

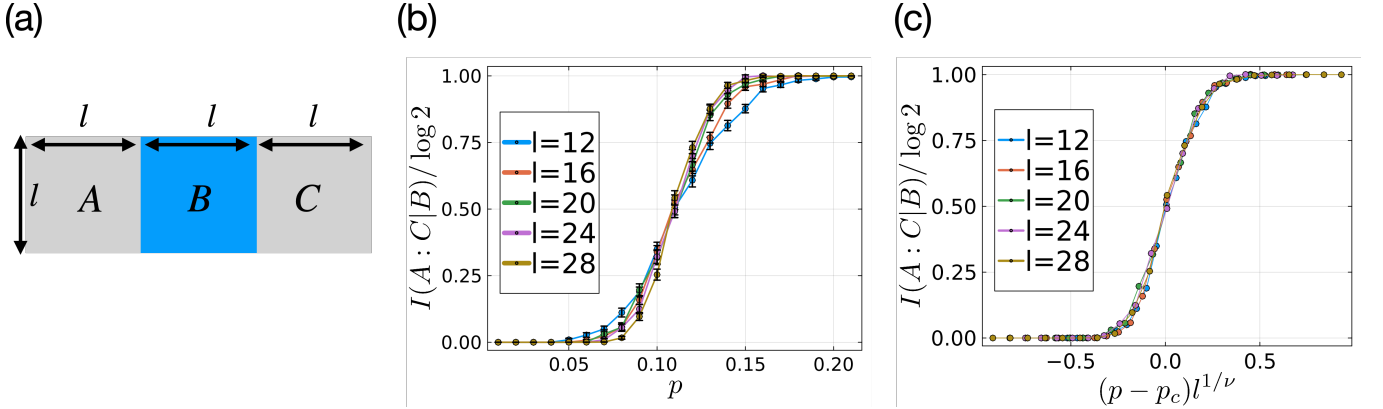


FIG. 7. (a) An alternate geometry used to compute the CMI of the trivial-to-SWSSB transition (in contrast, in the main text we used the geometry in Fig.1(a)). (b) The CMI as a function of  $p$  for various values of  $l$ . (c) Data collapse using the scaling ansatz  $I = f[(p - p_c)l^{1/\nu}]$  with  $p_c = 0.109$  and  $\nu = 1.5$